DOI:10.1021/jf902768v

JOURNAL OF AGRICULTURAL AND FOOD CHEMISTRY
ARTICLE

Intermolecular Interactions during Complex Coacervation of Pea Protein Isolate and Gum Arabic

Shuanghui Liu,[†] Yuan-Long Cao,[†] Supratim Ghosh,[§] Dérick Rousseau,[§] Nicholas H. Low,[†] and Michael T. Nickerson*,[†]

[†]Department of Food and Bioproduct Sciences, University of Saskatchewan, 51 Campus Drive, Saskatoon, Saskatchewan, Canada S7N 5A8 and [§]Department of Chemistry and Biology, Ryerson University, 350 Victoria Street, Toronto, Ontario, Canada M5B 2K3

The nature of intermolecular interactions during complexation between pea protein isolate (PPI) and gum arabic (GA) was investigated as a function of pH (4.30−2.40) by turbidimetric analysis and confocal scanning microscopy in the presence of destabilizing agents (100 mM NaCl or 100 mM urea) and at different temperatures (6−60 °C). Complex formation followed two pH-dependent structure-forming events associated with the formation of soluble and insoluble complexes and involved interactions between GA and PPI aggregates. Complex formation was driven by electrostatic attractive forces between complementary charged biopolymers, with secondary stabilization by hydrogen bonding. Hydrophobic interactions were found to enhance complex stability at lower pH (pH 3.10), but not with its formation.

KEYWORDS: Pea protein isolates; gum arabic; complex coacervation; nature of interactions

INTRODUCTION

The admixture of proteins and polysaccharides is widely used by the food industry to control food structure and texture or in the development of novel biomaterials (*1*). Depending on the biopolymer and solvent conditions, protein−polysaccharide interactions may lead to either segregative or associative phase separation. The former arises when both biopolymers carry a similar net repulsive charge, resulting in protein- and polysaccharide-rich phases. The latter occurs when biopolymers carry an opposing net charge, leading to separation into biopolymer- and solvent-rich phases (*2*, *3*). Depending on the biopolymer characteristics (e.g., type, reactive groups, chain length, branching, flexibility, hydrophobicity, mixing ratio, and concentration) and solvent conditions (e.g., pH and salts), various degrees of interactions can ensue, leading in some cases to precipitation (*4*−*6*). Through parameter adjustment, the nature of noncovalent interactions (i.e., electrostatic forces, hydrophobic interactions, and hydrogen bonding) between biopolymers can be tailored to create complex structures with novel functionality (*4*).

Coacervate formation is driven by strong electrostatic attractive forces, which cause biopolymers to rearrange into complexes to entrap solvent, and is at thermodynamic equilibrium with the solvent-rich phase. During its formation, entropy associated with biopolymer flexibility and solvent mixing is reduced and counteracts the enthalpic contributions arising from the release of water and counterions during complexation (*1*, *7*−*9*). The role of non-Coulombic forces is less clear and often depends strongly on the biopolymers present (and their characteristics) and solvent conditions. In some cases, admixtures of proteins with highly charged polysaccharides have been found to initiate complex formation at pH > p*I*, when both biopolymers have a similar net charge. Typically, these cases are attributed to localized positively charged areas on the protein's surface (*10*, *11*); however, secondary effects of hydrogen bonding and hydrophobic interactions are less well understood.

Complex coacervation typically occurs over a narrow pH range, between the pK_a of reactive groups along the polysaccharide backbone and the isoelectric point (p*I*) of the protein (*12*, *13*). Although mechanisms underlying complex formation are not fully elucidated, it is widely believed to be associated with two pH-dependent structure-forming events, corresponding to the formation of both soluble and insoluble complexes (*13*, *14*). The formation of soluble complexes (pH_c) signifies the first experimentally detectable noncovalent interaction between biopolymers and is characterized by a slight increase in turbidity during acid titration. By further lowering the pH, soluble complexes increase in size and number as a result of nucleation and growth. This causes macroscopic changes in phase behavior (*13*, *14*), which leads to the formation of insoluble complexes (at $pH_{\phi 1}$) and a rapid rise in turbidity (*2*, *3*, *15*). Complex growth (and turbidity) increases to a maximum, corresponding to a pH at which biopolymer interactions reach an electrical equivalence point (denoted pH_{opt}). Complexes begin to disassociate at pH < pH_{opt}, as the reactive groups along the polysaccharide backbone become protonated. Complete dissolution of complexes occurs at $pH_{\phi 2}$, as both biopolymers carry a similar net charge.

In this paper, the nature of interactions involved with complexation of pea protein isolate (PPI) and gum arabic (GA) was explored in relation to their pH-dependent structure-forming events. Field peas (*Pisum sativum*) are dominated by two major globulin proteins, legumin (350−400 kDa) and vicilin (150 kDa),

*Corresponding author [telephone (306) 966-5030; fax (306) 966-8898; e-mail Michael.Nickerson@usask.ca].

 Published on Web 11/25/2009

which are typically extracted using a pH-salt protocol to yield an isolate. In contrast, GA is an anionic carboxylated polysaccharide composed of three fractions: (a) a galactopyranose (galactan) polysaccharide backbone with branched side chains of β-(1→6) galactopyranose (~89%) with terminating residues of arabinose, glucuronic acid, and/or 4-*O*-methylglucuronic acid; (b) a covalently linked arabinogalactan−protein complex (~10%); and (c) a glycoprotein complex (~1%) (*16*).

Our group (*17*) studied the effect of pH, biopolymer mixing ratio, and salt on complex formation between PPI and GA polysaccharides. We found that optimal conditions for coacervation occurred at a 2:1 protein−polysaccharide mixing ratio in the absence of added salt and at a pH of 3.60 (pH_{opt}). At this pH, biopolymer interactions were electrically equivalent with a net charge of zero (i.e., zeta potential = 0 mV). Our group also postulated that due to significant optical density within the homogeneous protein solution at pH > pH_c, complex formation involved interactions between GA and small protein−protein aggregates rather than individual protein molecules. As the pH was lowered below pH_{opt}, a significant shoulder emerged, followed by rapid dissolution of complex structures at $pH_{\phi 2}$. Within this study, we investigated the nature of Coulombic and non-Coulombic interactions on PPI−GA complexation by turbidimetric analysis in the presence of NaCl and urea and as a function of temperature. Whey protein−GA complexation was also studied on a limited basis for comparative purposes only.

MATERIALS AND METHODS

Materials. Pea flour (PF) (Fiesta Flour, lot F147X, 2008) and GA powder (gum arabic FT pre-hydrated, lot 11229, 2007) were donated by Parrheim Foods (Saskatoon, SK) and TIC Gums (Belcamp, MD), respectively. PPI was prepared according to the method of Liu et al. (*17*). To summarize, PF was dissolved in 0.1 M phosphate buffer (pH 8.00) containing 6.4% KCl at a ratio of 1:10 (w/v) and stirred at 500 rpm for 24 h at room temperature (23 °C), followed by centrifugation at 3840*g* for 20 min to remove insoluble residues. Desalting of the supernatant was performed through dialysis using Spectro/Por tubing of 6−8 kDa cutoff (Spectrum Medical Industries, Inc., Houston, TX) against Milli-Q water (refreshing every 30 min) at 4 °C until conductivity (Thermo Scientific, Waltham, MA) reached 2.1 mS/cm. The desalted supernatant was then freeze-dried (Labconco Corp., Kansas City, MO) and stored at 4 °C. Proximate analyses on PF, PPI, and GA were carried out according to AOAC methods: 925.10 (moisture), 923.03 (ash), 920.87 (crude protein), and 920.85 (lipid). Carbohydrate content was determined on the basis of percent differential from 100%. PF was composed of 7.80% moisture, 21.78% protein (% N × 6.25), 1.00% lipid, 65.26% carbohydrate, and 4.16% ash; PPI contained 8.92% moisture, 82.80% protein, 1.06% lipid, 0.75% carbohydrate, and 6.47% ash; and GA consisted of 9.56% moisture, 0.86% protein, 0.11% lipid, 84.28% carbohydrate, and 5.19% ash. Whey protein concentrate (WP) (LE 006-6-280) (80% protein) was kindly donated by Davisco Foods International Inc. (Le Sueur, MN) for this study. Biopolymer concentrations used were based on protein and/or carbohydrate content in PPI, WP, or GA.

Turbidimetric Analysis. PPI, WP, and GA stock solutions (0.5% w/w; pH 8.00) were prepared by dissolving each powder in Milli-Q water under stirring (500 rpm) for 2 h at room temperature and then overnight at 4 °C to enhance hydration. Mixtures of PPI and GA (or WP and GA) were prepared by first diluting and then mixing the stock solutions at a 2:1 protein−GA mixing ratio and a total biopolymer concentration of 0.05% (w/w). Mixing conditions reflected earlier findings by Liu et al. (*17*), which were found to be optimal for PPI−GA coacervation. Changes to the pH-dependent turbidity profile during PPI−GA coacervation (at room temperature, 22−23 °C) were investigated in the presence of destabilizing agents and as a function of temperature to discern the nature of interactions involved with complex formation. A turbidimetric analysis of the WP−GA mixture was also performed at room temperature without the addition of destabilizing agents for comparative purposes only.

Turbidimetric titration upon acidification was measured using a UV−vis spectrophotometer (Mecasys Co., Daejeon, South Korea) at 600 nm using plastic cuvettes (1 cm path length), from pH 6.00 to 1.50 (*17*). The mixture was acidified by the addition of 0.05% (w/w) glucono-δ-lactone to bring the pH to 3.90, followed by the dropwise addition of HCl (gradient HCl concentration based on pH: 0.05 M > pH 3.30; 0.5 M > pH 2.70; 1 M > pH 2.20; 2.0 M > pH 1.50). Dilution effects and changes to solution conductivity were considered to be minimal, as described by Liu et al. (*17*). Critical pH values (pH_c, $pH_{\phi 1}$, pH_{opt}, $pH_{\phi 2}$) associated with structure-forming events were determined graphically according to the methods of Weinbreck et al. (*11*) and Liu et al. (*17*). Changes to the pH-dependent turbidity profiles of PPI−GA mixtures, measured at room temperature, were investigated in the presence of 100 mM NaCl and 100 mM urea and as a function of temperature (6, 45, and 60 °C). Sample temperatures at 45 and 60 °C were maintained using a water bath; while those at 6 °C were made by storing the samples at this temperature and by placing the instrument within a walk-in cold room maintained at 6 °C. Homogeneous PPI, WP, and GA solutions were used as blanks at their respective concentrations for all solution conditions tested. All measurements were made in triplicate.

Confocal Laser Scanning Microscopy (CLSM). Fluorescence microscopy was used to characterize PPI−GA complexation at pH 4.30, 4.00, 3.70, 3.60, 3.10, and 2.40 at room temperature and at pH 3.10 and 2.40 at 60 °C. Rhodamine B (Sigma-Aldrich, Oakville, ON) (0.01%, w/w) was used to stain the aqueous dispersion (maximum excitation and emission at 543 and 567 nm, respectively). Samples were placed on viewing slides (Fisher Scientific Ltd., Ottawa, ON), covered with a coverslip (Fisher Scientific Ltd.), and then transferred to the stage (at room temperature) of an upright Zeiss LSM-510 confocal laser scanning microscope (Zeiss Inc., Toronto, ON) used in the fluorescence mode. Measurements made at 60 °C, involved preheating the samples, slides, and coverslips and the use of a Peltier-controlled temperature stage (Instec, Boulder, CO) mounted on the microscope. The actual temperature on the slide was measured by a thin-wire digital thermocouple (K-type; Omega, Montréal, PQ), and the stage temperature was adjusted accordingly so that the temperature of the sample on the slide remained at 60 °C throughout the experiment. Images were collected using a 543 nm laser, a long pass 560 nm filter, and a Plan-Apochromat 20× lens with a numerical aperture of 0.75. The images were processed with LSM 510 Image Analysis software (v3.2 Zeiss Inc.).

Statistical Analysis. A one-way analysis of variance (ANOVA) with a Scheffe post hoc test was used to measure statistical differences between critical pH values (pH_c, $pH_{\phi 1}$, pH_{opt}, and $pH_{\phi 2}$) in the presence and absence of destabilizing agents and as a function of temperature. All statistical analyses were performed using Systat software (SPSS Inc., ver. 10, 2000, Chicago, IL).

RESULTS AND DISCUSSION

Complex Coacervation of Pea Protein Isolate and Gum Arabic. Complex coacervation in mixtures of PPI and GA was studied during acid titration for a 2:1 PPI−GA weight-mixing ratio. At pH > 5.60 [p*I* of PPI (*17*)], biopolymers carried a similar net charge and repelled one another. Due to the dilute nature of the system, the PPI and GA molecules remained cosoluble. At pH < 5.60, biopolymers carried opposing net charges and began to attract one another. Complex coacervation is thought to occur through two structure-forming events associated with the formation of soluble (pH_c) and insoluble ($pH_{\phi 1}$) complexes at pH 4.23 and 3.77, respectively (**Figure 1**). At pH < $pH_{\phi 1}$, the solution underwent a transparent-to-cloudy transition, as evidenced by the significant rise in optical density (OD) to a maximum of 1.320, at which significant PPI−GA interactions occurred (pH_{opt} 3.60) (**Figure 1**). At pH < pH_{opt}, the stability of the PPI−GA complexes was reduced due to the progressive protonation of the carboxyl groups along the GA backbone during acid titration. Dissolution of the formed complexes occurred at $pH_{\phi 2}$ (pH 2.55), at which both biopolymers again carried a similar net charge (**Figure 1**). Under the same conditions, scattering intensities for

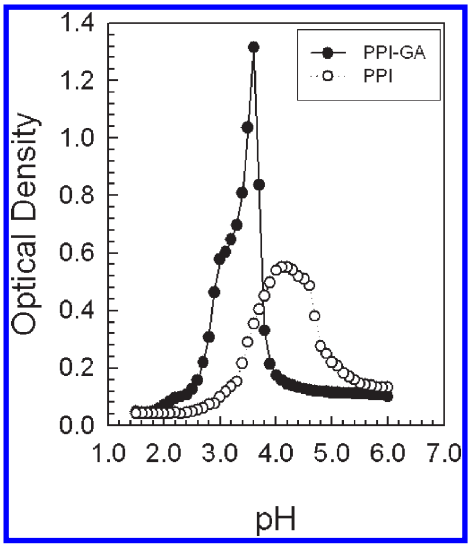

Figure 1. Turbidity curves of homogeneous and mixed (2:1 ratio) PPI−GA systems as a function of pH.

GA solutions were absent (not shown). In contrast, significant scattering intensities were seen for PPI alone over a pH range of 3.20−5.50, reaching a maximum OD of ~0.55 at pH 4.30, before declining at higher pH (i.e., pH >4.60). Complexes are thought to form through the interactions of GA chains with protein−protein aggregates rather than individual proteins, because the mixed and homogeneous PPI turbidity curves overlapped within the pH range of 3.20−4.00 (**Figure 1**). Laos et al. (*7*) found a similar turbidimetric behavior while studying complexation of furcellaran with bovine serum albumin and β-lactoglobulin, noting that the furcellaran−protein complexes were much larger than the protein aggregates alone.

The lack of scattering intensity in the mixed system over the pH range of 5.50−4.23 relative to the PPI alone (**Figure 1**) suggests that electrostatic repulsive forces are still prevalent even at pH < p*I* of the protein and that complex structures are either absent or very small in nature. The suppression of structure formation was confirmed by CLSM, where at pH 4.30 PPI aggregates were greater in size and number (**Figure 2a**) than in the mixed system (**Figure 2b**). In the case of PPI alone, aggregate size and number declined as the pH was lowered from 4.30 to 4.00 (**Figure 2a**,**c**) and was absent at pH <4.00 (not shown). In the mixed system, small aggregates were apparent at pH 4.30 (pH > pH_c), supporting the hypothesis that protein−protein aggregates play a role in complex formation (**Figure 2b**). As the pH was lowered to 4.00 (soluble complexes were present; pH < pH_c), 3.70 (insoluble complexes were present; pH < $pH_{\phi 1}$), and then 3.60 (pH_{opt}), complexes grew in size and number (**Figure 2d**−**f**). This trend reflects progressive charge neutralization due to complexation leading to pH_{opt}, at which maximum complex instability, charge neutralization, insolubility, and concentration occur. Structures were irregular in shape, were polydisperse, and appeared to consist of multiple subunits. Under these conditions, the spatial distribution of PPI versus GA could not be determined within the complex structure, as the GA chains were too small to resolve (~200−250 nm). Observed structures in the mixture at pH < pH_c are assumed to be composed of GA−pea protein aggregates. At pH < pH_{opt}, the size and number of complexes were reduced until becoming negligible in size at pH 2.10 (pH < $pH_{\phi 2}$) (**Figure 2g**,**h**).

Turbidimetric analysis of the PPI−GA mixture at pH < pH_{opt} revealed the presence of a pronounced shoulder at pH 2.80−3.20, which was absent for a whey protein (WP)−GA mixture under

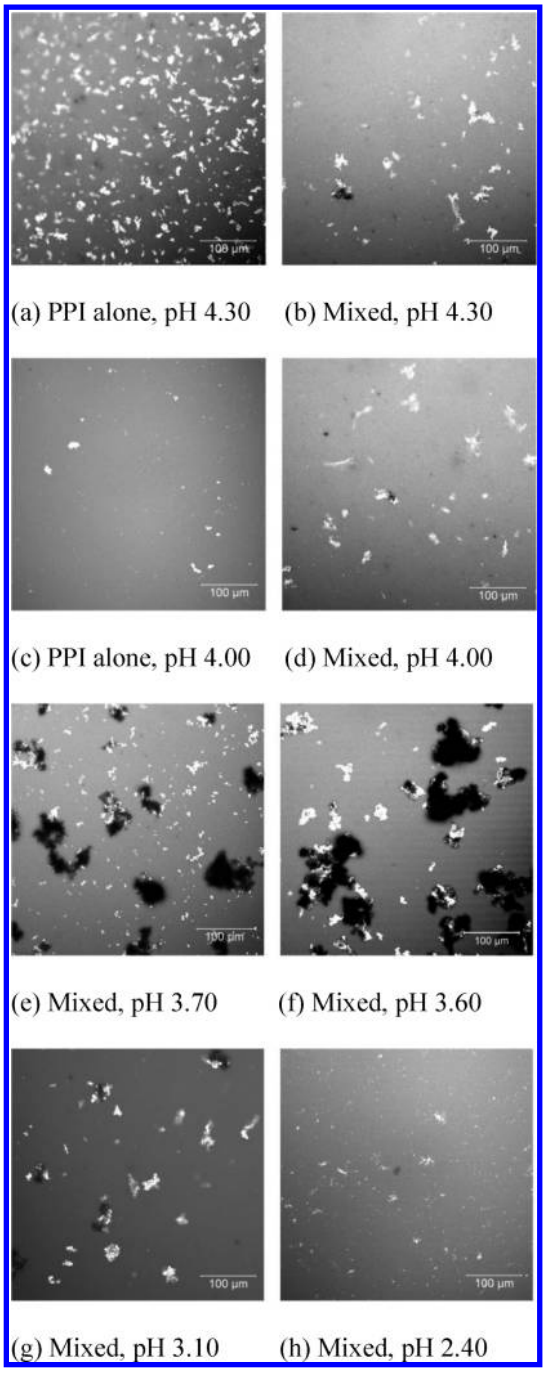

Figure 2. Microstructures obtained by confocal laser scanning microscopy of homogeneous and mixed (2:1 ratio) PPI−GA systems taken at room temperature as a function of pH: (**a**) PPI alone, pH 4.30; (**b**) mixed, pH 4.30; (**c**) PPI alone, pH 4.00; (**d**) mixed, pH 4.00; (**e**) mixed, pH 3.70; (**f**) mixed, pH 3.60; (**g**) mixed, pH 3.10; (**h**) mixed, pH 2.40.

the same conditions (**Figure 3**). Inhibition of the dissolution of PPI−GA complexes at these pH values may be the result of prevalent hydrophobic interactions that stabilize the PPI aggregates and counteract Coulombic forces. Knowledge of the role of protein−protein aggregates in complex coacervation is somewhat limited in the literature and typically restricted to smaller milk-based proteins. Sanchez et al. (*6*), Schmitt et al. (*18*), and Sanchez and Renard (*19*) found that protein−protein aggregates play a significant stabilization role in β-lactoglobulin−acacia gum complexation relative to aggregate-free mixtures.

Effect of Destabilizing Agents on Complex Formation. Complex formation in admixtures of PPI and GA was also studied in the

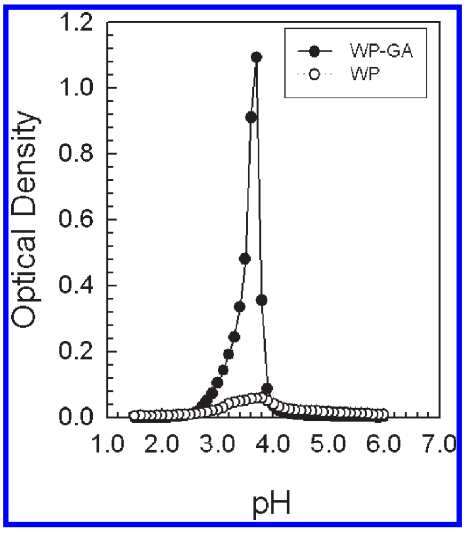

Figure 3. Turbidity curves of homogeneous and mixed (2:1 ratio) WP−GA systems as a function of pH.

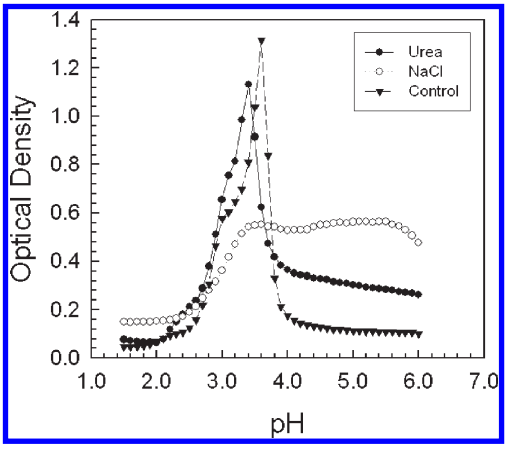

Figure 4. Turbidity curves of a PPI−GA mixture (2:1 ratio) as a function of pH, with (100 mM NaCl; 100 mM urea) and without destabilizing agents (control).

presence of 100 mM NaCl and urea by turbidimetric analysis and contrasted with the same system in the absence of destabilizing agents. Urea acts to disrupt both hydrogen bonding and hydrophobic interactions (*20*), whereas the presence of ions acts to screen charged reactive sites on both biopolymers to disrupt intermolecular electrostatic interactions. PPI−GA complexation was found to be inhibited in the current study with the addition of NaCl, as Na^+ and Cl^- ions acted to screen charges on GA and PPI molecules so as to disrupt electrostatic attractive forces between the biopolymers (*11*) (**Figure 4**). In contrast, the addition of urea caused a shift in critical pH values (pH_c, $pH_{\phi 1}$, and pH_{opt}) to lower pH values relative to the control ($p < 0.05$), as hydrogen bonding was reduced (**Figure 4**). Specifically, pH_c, $pH_{\phi 1}$, and pH_{opt} were reduced from 4.23, 3.77, and 3.60 (without destabilizing agents) to 3.98, 3.63, and 3.40 in the presence of 100 mM urea, respectively. Results suggest that complex formation between PPI and GA is primarily driven by electrostatic attractive forces, with secondary stabilization arising from hydrogen bonding. Girard et al. (*10*) found that pH_c for β-lactoglobulin and high-methylated pectin mixtures shifted from 6.1 to 5.5 in the presence of 110 mM NaCl, highlighting the role of electrostatic forces on complex formation. In contrast, no effect on pH_c was observed in the presence of urea, but complex yield was reduced. Lii and coworkers (*21*) found that 7 M urea increased the solubility of

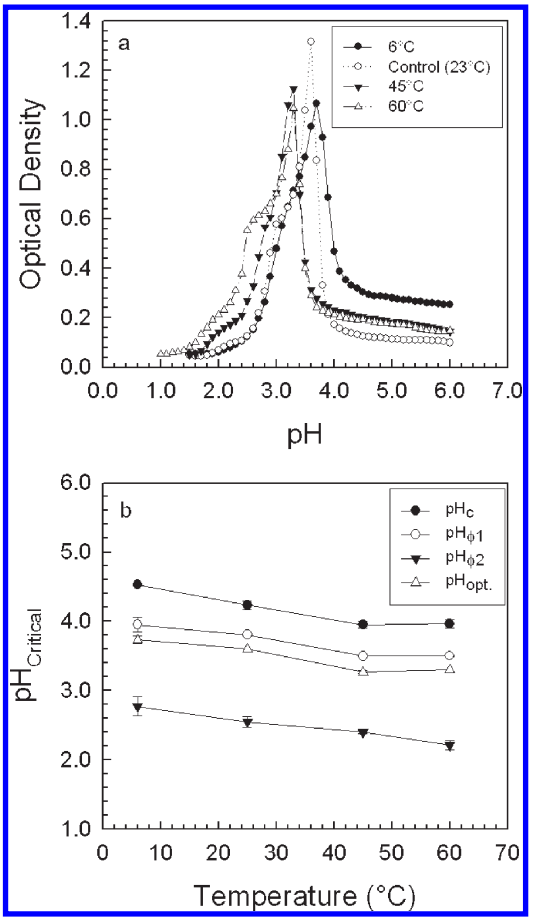

Figure 5. (**a**) Turbidity curves for a PPI−GA mixture (2:1 ratio) as a function of pH and temperature. (The control turbidity profile was maintained at room temperature, 23 °C.) (**b**) Phase diagram of critical pH values associated with structure-forming events for a 2:1 PPI−GA mixed system as a function of temperature ($n = 3$).

xanthan gum−gelatin complexes, suggesting that both hydrogen bonding and electrostatic interactions contributed to complexation. Antonov and Sochinsky (*22*) found non-Coulombic interactions were occurring in alfalfa rubisco and pectin mixtures under neutral or slightly alkaline pH values, which they attributed to hydrogen bonding between these molecules.

Effect of Temperature on Complex Formation. The effect of temperature on PPI−GA complex formation was studied over a temperature range of 6−60 °C relative to a PPI−GA control, which was maintained at room temperature. In general, the extent of hydrogen bonding increases at lower temperatures, whereas at higher temperatures, hydrophobic interactions become more prevalent (*11*). As the temperature was lowered from 23 to 6 °C, a shift in the turbidity profile (**Figure 5a**) and critical pH values (**Figure 5b**) toward higher pH values occurred ($p < 0.05$), which was a consequence of improved complex stability by hydrogen bonding. As temperatures were elevated relative to the control, turbidity profiles and critical pH values shifted to lower pH values ($p < 0.05$) (**Figure 5**). This shift was postulated to be attributable to the decline in hydrogen bonding at elevated temperatures as the complexes destabilized. Weinbreck and coworkers (*11*) reported that $pH_{\phi 1}$ increased slightly at lower temperatures in whey protein−λ-carrageenan mixtures. Girard et al. (*10*) reported that at elevated temperatures, the yield of β-lactoglobulin and high-methylated pectin complexes declined, suggesting that hydrogen bonding was involved with complex formation. In contrast, Singh et al. (*5*) did not observe any

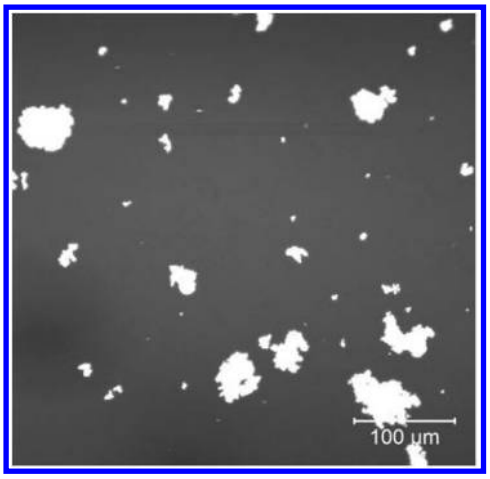

Figure 6. Microstructures obtained by confocal laser scanning microscopy of an aqueous mixture of PPI and GA taken at 60 °C at pH 3.10.

temperature variation of pH_c and $pH_{\phi 1}$ over the range of 25−50 °C during gelatin−agar complexation.

Although hydrophobic interactions did not appear to influence complex formation, they did play a role in the stability of the PPI−GA complexes, especially at low pH (pH 3.10). On the basis of turbidimetry, the shoulder found at $pH < pH_{opt}$ in the control became progressively more pronounced as temperatures were raised (**Figure 5a**), suggesting that hydrophobic interactions within the protein−protein aggregates were becoming more dominant. This phenomenon also corresponded to larger complex structures observed at 60 °C at pH 3.10 by CLSM (**Figure 6**) relative to those of the control maintained at room temperature (**Figure 2g**). The sizes of the complexes at both temperatures were similar at pH 2.40 (not shown).

Complex formation involving PPI and GA occurred over a very narrow pH range and involved interaction between GA molecules and PPI aggregates. The nature of interactions involved in their coacervation was dominated by electrostatic attractive forces with secondary stabilization by hydrogen bonding. In contrast, hydrophobic interactions appeared to become more prevalent at $pH < pH_{opt}$ when the strength of Coulombic forces started to diminish, suggesting their role might be associated with complex stability rather than formation.

Note Added after ASAP Publication

Due to a production error, Figure 1 was modified in the version of this paper published ASAP November 25, 2009; the corrected version published ASAP December 1, 2009.

LITERATURE CITED

(1) Singh, S. S.; Bohidar, H. B.; Bandyopadhyay, S. Study of gelatin−agar intermolecular aggregates in the supernatant of its coacervate. *Colloids Surf. B: Biointerfaces* **2007**, *57*, 29–36.

(2) deKruif, C. G.; Tuinier, R. Polysaccharide protein interactions. *Food Hydrocolloids* **2001**, *15*, 555–563.

(3) Turgeon, S. L.; Beaulieu, M.; Schmitt, C.; Sanchez, C. Protein−polysaccharide interactions: phase-ordering kinetics, thermodynamic and structural aspects. *Curr. Opin. Colloid Interface Sci.* **2003**, *8*, 401–414.

(4) McClements, D. J. Non-covalent interactions between proteins and polysaccharides. *Biotechnol. Adv.* **2006**, *24*, 621–625.

(5) Singh, S. S.; Siddhanta, A. K.; Meena, R.; Prasad, K.; Bandyopadhyay, S.; Bohidar, H. B. Intermolecular complexation and phase separation in aqueous solutions of oppositely charged biopolymers. *Int. J. Biol. Macromol.* **2007**, *41*, 185–192.

(6) Sanchez, C.; Mekhloufi, G.; Renard, D. Complex coacervation between β-lactoglobulin and acacia gum: a nucleation and growth mechanism. *J. Colloid Interface Sci.* **2006**, *299*, 867–873.

(7) Laos, K.; Brownsey, G. J.; Ring, S. G. Interactions between furcellaran and the globular proteins bovine serum albumin and β-lactoglobulin. *Carbohydr. Polym.* **2007**, *67*, 116–123.

(8) Schmitt, C.; Sanchez, C.; Desobry-Banon, S.; Hardy, J. Structure and technofunctional properties of protein-polysaccharide complexes: a review. *Rev. Food Sci. Nutr.* **1998**, *38*, 689–753.

(9) Ye, A. Complexation between milk proteins and polysaccharides via electrostatic interactions: principles and applications − a review. *Int. J. Food Sci. Technol.* **2008**, *43*, 406–415.

(10) Girard, M.; Turgeon, S. L.; Gauthier, S. F. Interbiopolymer complexing between β-lactoglobulin and low- and high-methylated pectin measured by potentiometric titration and ultrafiltration. *Food Hydrocolloids* **2002**, *16*, 585–591.

(11) Weinbreck, F.; Nieuwenhuijse, H.; Robijn, G. W.; de Kruif, C. G. Complexation of whey proteins with carrageenan. *J. Agric. Food Chem.* **2004**, *52*, 3550–3555.

(12) Weinbreck, F.; de Vries, R.; Schrooyen, P.; de Kruif, C. G. Complex coacervation of whey proteins and gum arabic. *Biomacromolecules* **2003**, *4*, 293–303.

(13) Ducel, V.; Richard, J.; Saulnier, P.; Popineau, Y.; Boury, F. Evidence and characterization of complex coacervates containing plant proteins: application to the microencapsulation of oil droplets. *Colloids Surf. A: Physicochem. Eng. Aspects* **2004**, *232*, 239–247.

(14) Girard, M.; Sanchex, C.; Laneuville, S. I.; Turgeon, S. K.; Gauthier, S. F. Associative phase separation of β-lactoglobulin/pectin solutions: a kinetic study by small angle static light scattering. *Colloids Surf. B: Biointerfaces* **2004**, *35*, 15–22.

(15) Weinbreck, F.; Nieuwenhuijse, H.; Robijn, G. W.; de Kruif, C. G. Complex formation of whey proteins: exocellular polysaccharide EPS B40. *Langmuir* **2003**, *19*, 9404–9410.

(16) Dror, Y.; Cohen, Y.; Yerushalmi-Rozen, R. Structure of gum arabic in aqueous solution. *J. Polym. Sci., Part B: Polym. Phys.* **2006**, *44*, 3265–3271.

(17) Liu, S.; Low, N. H.; Nickerson, M. T. Effect of pH, salt, and biopolymer ratio on the formation of pea protein isolate−gum arabic complexes. *J. Agric. Food Chem.* **2009**, *57*, 1521–1526.

(18) Schmitt, C.; Sanchez, C.; Despond, S.; Renard, D.; Thomas, F.; Hardy, J. Effect of protein aggregates on the complex coacervation between β-lactoglobulin and acacia gum at pH 4.2. *Food Hydrocolloids* **2000**, *14*, 403–413.

(19) Sanchez, C.; Renard, D. Stability and structure of protein−polysaccharide coacervates in the presence of protein aggregates. *Int. J. Pharm.* **2002**, *242*, 319–324.

(20) Uruakpa, F. O.; Arntfield, S. D. Impact of urea on the microstructure of commercial canola protein-carrageenan network: a research note. *Int. J. Biol. Macromol.* **2006**, *38*, 115–119.

(21) Lii, C. Y.; Liaw, S. C.; Lai, V. M.-F.; Tomasik, P. Xanthan gum−gelatin complexes. *Eur. Polym. J.* **2002**, *38*, 1377–1381.

(22) Antonov, Y. A.; Soshinsky, A. Interactions and compatibility of ribuloso-1,5-bisphosphate carboxylase/oxygenase from alfalfa with pectin in aqueous medium. *Int. J. Biol. Macromol.* **2000**, *27*, 279–285.

Received for review August 7, 2009. Revised manuscript received November 11, 2009. Accepted November 12, 2009. Financial assistance for this study was provided by the Natural Science and Engineering Research Council of Canada and the Advanced Foods and Materials Network.